Surg Radiol Anat (2012) 34:235–247
DOI 10.1007/s00276-011-0870-2

ORIGINAL ARTICLE

Outlining of the detailed structures in sectioned images from Visible Korean

Dong Sun Shin · Jin Seo Park · Hyo Seok Park · Sung Bae Hwang · Min Suk Chung

Received: 16 March 2011 / Accepted: 6 September 2011 / Published online: 25 September 2011

Abstract
Purpose Sectioned images of cadavers enable creation of realistic three-dimensional (3D) models. In order to build a 3D model of a structure, the structure has to be outlined in the sectioned images. The outlining process is time consuming; therefore, users want to be provided with outlined images. The more detailed structures are outlined, the greater potential for wider application of the outlined images.
Methods In the Visible Korean, sectioned images (intervals 0.2 mm) of the entire body of a male cadaver were prepared. In the available 1,702 sectioned images (intervals 1 mm), 937 structures were outlined over a period of 8 years. The outlined images were altered to black-filled images for each structure; black-filled images were selected for distribution in order to maintain small file sizes.
Results We attempted to determine whether black-filled images could be used in various situations. The outlines of these images were interpolated for production of new images at 0.2 mm intervals. The outlines were then filled with different colors for construction of color-filled images of all structures. Volume and surface reconstructions of the black-filled images were executed in order to build volume and surface models.
Conclusion The black-filled images with corresponding sectioned images presented here are the source of realistic 3D models for use in medical simulation systems.

Keywords Visible Human Projects · Cadaver · Frozen sections · Computer-assisted image processing · Three-dimensional imaging

D. S. Shin · M. S. Chung (✉)
Department of Anatomy, Ajou University School of Medicine, Worldcup-ro 164, Suwon 443-749, Republic of Korea
e-mail: dissect@ajou.ac.kr

J. S. Park · H. S. Park
Department of Anatomy, Dongguk University College of Medicine, 707 Seokjang-dong, Gyeongju 780-714, Republic of Korea

S. B. Hwang
Department of Physical Therapy, Kyungbuk College, Youngju 750-712, Republic of Korea

Introduction

Serially sectioned images of cadavers can be used for production of realistic three-dimensional (3D) models. Such sectioned images show true human body colors in high resolution; this feature differentiates these images from other alternatives, such as CT and MR images [1, 18, 19, 21, 26]. Nevertheless, the sectioned images themselves are not sufficient; in order to construct 3D models of body structures for use in medical simulation systems, the structures must be outlined in the sectioned images; this process is very time consuming. Therefore, providing detailed outlined images would allow wider availability of image data for use in medical applications [8, 17, 24, 25].

In the Visible Human Project, Chinese Visible Human, and Virtual Chinese Human, outlined images were constructed mainly by the principal investigators of the projects [4, 7, 10, 17, 20, 23, 25]. However, information regarding which structures appeared in the outlined images, how the structures were outlined on the computer used, which file format was used, and how the outlined images were distributed to the public was not fully reported. Therefore, only the developers know the details of the images, and use of the images is restricted to them.

In the Visible Korean data set, sectioned images (intervals 0.2 mm) were acquired of an entire male cadaver. A total of 1,702 sectioned images (intervals of 1 mm) were selected for outlining. Our challenge was to outline as many structures of the entire body as we could identify in the sectioned images. Consequently, from early 2002 to late 2009 (8 years), approximately 900 structures were outlined by medical experts. The outlining was performed interactively on Photoshop (CS3 version 10; Adobe Systems, Inc., San Jose, CA, USA) in order to produce 1,702 Photoshop data (PSD) files, namely outlined images of all structures. Each PSD file was composed of approximately 900 layers, each of which contained outlines of individual structures [12]. However, these layers were too numerous to handle; thus, we converted these PSD files into TIFF (tagged image file format) files, which were black-filled images of each structure. Then, volume and surface reconstructions were attempted using the black-filled images in order to demonstrate their potential as distributed data.

The objective of this research was to present black-filled images of many body structures, along with the corresponding sectioned images from the Visible Korean project. The hope is that these images will encourage other investigators to construct 3D models that can be used in medical learning and clinical practice.

Materials and methods

In addition to the basic necessity for outlined images that correctly reflect human anatomy, there are two additional requirements. Suppliers of outlined images should develop a system that automates the outlining required without the need for programming, and those who will use the images must be able to obtain and apply the images easily [12]. To achieve these goals, we have performed trials for determination of how to facilitate this process.

Outlining

We obtained 8,506 sectioned images (0000.tif, 0001.tif,…, 8505.tif) of a male cadaver at 0.2 mm intervals with 0.2 mm pixels in 24-bit color (Fig. 1a). To ensure good quality of the images, a young adult cadaver (33 years old) without obesity (height, 1.65 m; weight, 55 kg) was selected for the final collection of data. The subject died of leukemia, which caused pneumonia and splenomegaly. However, the drawback included just limited sections of the whole body [13]. From these sectioned images, we selected 1,702 images (0000.tif, 0005.tif,…, 8505.tif) taken at 1 mm intervals for outlining; the outlining at an initial 0.2 mm intervals required intensive labor.

Evaluation of the sectioned images was performed by medical experts who decided on the structures that would be outlined. Important structures (e.g., coronary arteries) were included, although they were unclear in the sectioned images. Where unclear, these images were printed out on paper; complicated structures were outlined and annotated by pen. This aided in decisions regarding whether the structures would be outlined by computer [16]. Bilateral symmetric structures (e.g., right and left first ribs) were outlined individually and individually counted. Consequently, the decision was made to outline 937 structures. These structures were categorized according to systems; further classifications, orders, names, and abbreviations of the structures were used as defined by the Terminologia Anatomica (Table 1) [3].

Tubular-like structures with walls and lumina were outlined in three ways. Because the luminal contours of structures such as the small intestine and urogenital tract were too narrow to be identified, the outlines were drawn along their mural contours. On the other hand, the outline of the respiratory tract and blood vessels was drawn along the luminal contours, which were more distinct than the mural contours. Outlining along the luminal contours might be used for virtual endoscopy systems in order to illustrate the true colors of the inside of luminal structures [14]. The walls and lumina of structures like the stomach and urinary bladder were large and obvious; therefore, they were outlined along both the mural and luminal contours (Table 1).

On Photoshop, the sectioned images were saved as PSD files (0000.psd, 0005.psd,…, 8505.psd). In each PSD file, 937 layers, which were named according to the structure, were created (Table 1), even though many of the layers did not include the structures' outlines. That is, only PSD files with complete layers could be automatically transformed into black-filled images, in the next step [12].

Sometimes, in Photoshop, the 'sharpen' filter was applied in order to make a structure's border clearer, or the 'median' filter was used to generate the structure's color with less noise. Structures were outlined automatically using the 'magic wand' tool, semi-automatically using the 'quick selection' or 'magnetic lasso' tool, or manually using the 'lasso' tool in sequence (Fig. 2b). Outlines of each structure were placed on the layers of the structure [12].

Information on the 937 outlined structures is provided in Table 2, including each structure's name and side (in the case of symmetrical bilateral structures), top image, bottom image, and red, green, and blue (RGB) triplets. For example, the cranium without the mandible was outlined in 0035.psd, 0040.psd,…, 1010.psd (196 images). In the latter procedure, the RGB triplet was drawn for filling in the

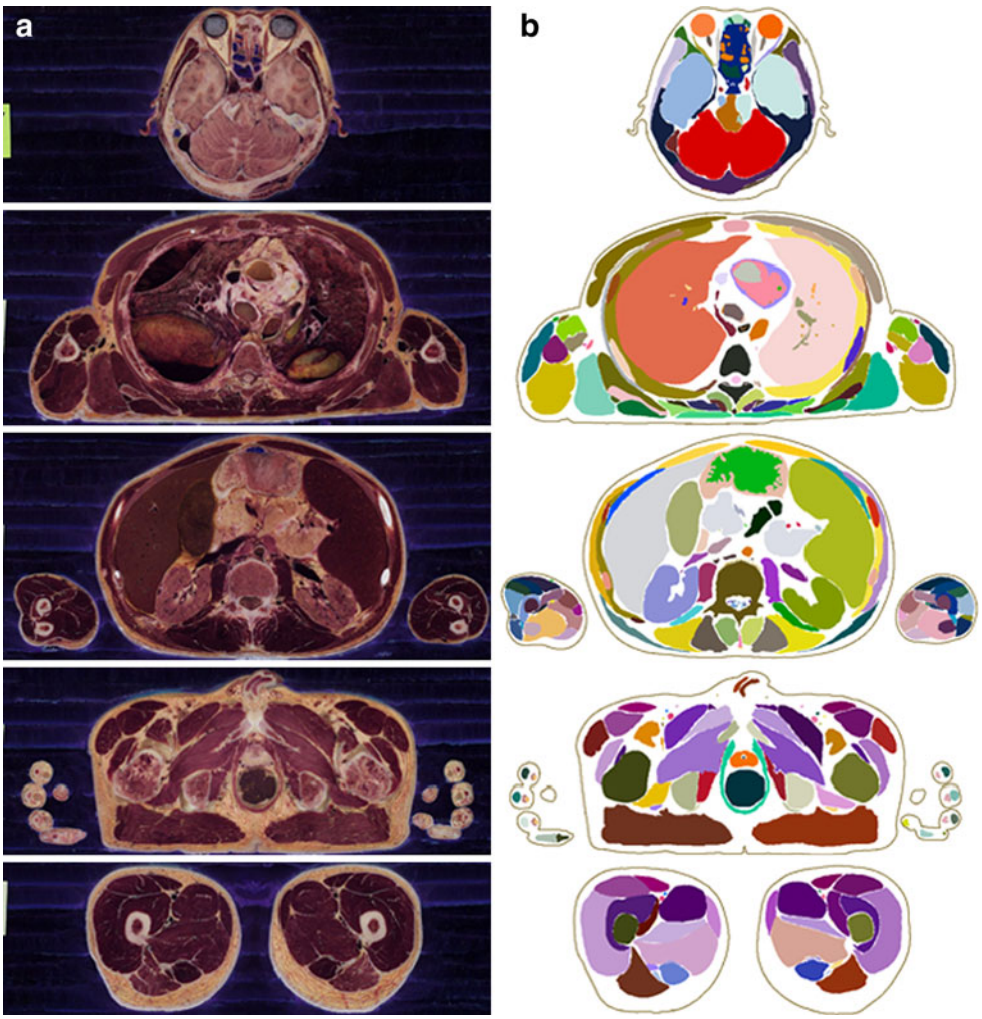

Fig. 1 **a** Sectioned images and **b** *color-filled* images of the body of the Visible Korean

outlines with colors. The RGB triplet was allocated differently among neighboring structures.

Filling outlines of each structure with black

Outlines of each structure were separated automatically using the layers in the PSD files; the outlines were then filled in order to produce black-filled images (TIFF files). Unlike outlined images, the black-filled images did not involve sectioned images (Fig. 2c). The color depth was changed from a 24-bit color to a 2-bit (binary) color in order to reduce the file size. In the case of the cranium without a mandible, 196 black-filled images (0035.tif, 0040.tif,…, 1010.tif) were constructed and were moved to the 'Cranium without mandible' folder (Table 2). A total of 937 folders (with the names of structures) were created in advance on a computer hard disk (Table 1).

The featureless black-filled images, which we planned to make available, have many applications. We assessed potential applications as follows.

Interpolating outlines

The intervals (1 mm) of black-filled images did not fit into the original intervals (0.2 mm) of sectioned images, and, thus, the 8,506 sectioned images could not be used to build fine volume models of structures with 0.2 mm voxels. In this study, we tried to construct black-filled images at 0.2 mm intervals by interpolation.

On Photoshop, from the black-filled images (TIFF files) of a portion of the spleen, outlined images (PSD files) were acquired automatically using the 'magic wand' tool, a reversal of the process (Fig. 3a). The outlined images were imported on Combustion (version 4; Autodesk, Inc., San Rafael, CA, USA), and semiautomatic interpolation was then performed using the 'animate' tool for creation of additional intervening outlines at 0.2 mm intervals (Fig. 3b). In cases where the created outlines did not fit the structures, the outlines were manually modified by moving their anchor and control points. Subsequently, the new outlined images were transformed into black-filled images [16].

Table 1 Nine-hundred and thirty-seven outlined structures

System	Classification	Structure
Skeletal (191)	Cranium	Cranium without mandible, parietal bone, frontal bone, occipital bone, temporal bone, ethmoid bone, crista galli, lacrimal bone*, nasal bone, maxilla, zygomatic bone*, mandible
	Vertebral column	First cervical vertebra, second cervical vertebra, third cervical vertebra, fourth cervical vertebra, fifth cervical vertebra, sixth cervical vertebra, seventh cervical vertebra, first thoracic vertebra, second thoracic vertebra, third thoracic vertebra, fourth thoracic vertebra, fifth thoracic vertebra, sixth thoracic vertebra, seventh thoracic vertebra, eighth thoracic vertebra, ninth thoracic vertebra, tenth thoracic vertebra, eleventh thoracic vertebra, twelfth thoracic vertebra, first lumbar vertebra, second lumbar vertebra, third lumbar vertebra, fourth lumbar vertebra, fifth lumbar vertebra, sacrum, coccyx
	Thoracic skeleton	First rib*, second rib*, third rib*, fourth rib*, fifth rib*, sixth rib*, seventh rib*, eighth rib*, ninth rib*, tenth rib*, eleventh rib*, twelfth rib*, sternum
	Bones of upper limb	Scapula*, clavicle*, humerus*, radius*, ulna*, scaphoid*, lunate*, triquetrum*, pisiform*, trapezium*, trapezoid*, capitate*, hamate*, first metacarpal bone*, second metacarpal bone*, third metacarpal bone*, fourth metacarpal bone*, fifth metacarpal bone*, first proximal phalanx*, second proximal phalanx*, third proximal phalanx*, fourth proximal phalanx*, fifth proximal phalanx*, second middle phalanx*, third middle phalanx*, fourth middle phalanx*, fifth middle phalanx*, first distal phalanx*, second distal phalanx*, third distal phalanx*, fourth distal phalanx*, fifth distal phalanx*
	Bones of lower limb	Hip bone*, femur*, patella*, tibia*, fibula*, talus*, calcaneus*, navicular*, medial cuneiform*, intermediate cuneiform*, lateral cuneiform*, cuboid*, first metatarsal*, second metatarsal*, third metatarsal*, fourth metatarsal*, fifth metatarsal*, first proximal phalanx*, second proximal phalanx*, third proximal phalanx*, fourth proximal phalanx*, fifth proximal phalanx*, second middle phalanx*, third middle phalanx*, fourth middle phalanx*, fifth middle phalanx*, first distal phalanx*, second distal phalanx*, third distal phalanx*, fourth distal phalanx*, fifth distal phalanx*
Articular (52)	Vertebral joints	Interspinous ligament (L I–L II), interspinous ligament (L II–L III), interspinous ligament (L III–L IV), interspinous ligament (L IV–LV), interspinous ligament (L V–sacrum), ligamentum flavum (L I–L II), ligamentum flavum (L II–L III), ligamentum flavum (L III–L IV), ligamentum flavum (L IV–L V), ligamentum flavum (L V–sacrum), supraspinous ligament, anterior longitudinal ligament, posterior longitudinal ligament, intervertebral disc (C II–C III), intervertebral disc (C III–C IV), intervertebral disc (C IV–C V), intervertebral disc (C V–C VI), intervertebral disc (C VI–C VII), intervertebral disc (C VII–T I), intervertebral disc (T I–T II), intervertebral disc (T II–T III), intervertebral disc (T III–T IV), intervertebral disc (T IV–T V), intervertebral disc (T V–T VI), intervertebral disc (T VI–T VII), intervertebral disc (T VII–T VIII), intervertebral disc (T VIII–T IX), intervertebral disc (T IX–T X), intervertebral disc (T X–T XI), intervertebral disc (T XI–T XII), intervertebral disc (T XII–L I), intervertebral disc (L I–L II), intervertebral disc (L II–L III), intervertebral disc (L III–L IV), intervertebral disc (L IV–L V), intervertebral disc (L V–sacrum)
	Joints of lower limb	Sacrotuberous ligament*, sacrospinous ligament*, acetabular labrum*, transverse acetabular ligament*, ligament of head of femur*, lateral meniscus, medial meniscus, anterior cruciate ligament, posterior cruciate ligament, fibular collateral ligament, tibial collateral ligament

Table 1 continued

System	Classification	Structure
Muscular (266)	Muscles of head	Buccinator m.*, masseter m.*, temporal m.*, lateral pterygoid m.*, medial pterygoid m.*
	Muscles of neck	Longus colli m.*, longus capitis m.*, anterior scalene m.*, middle scalene m.*, posterior scalene m.*, sternocleidomastoid m.*, rectus capitis anterior m.*, rectus capitis lateralis m.*, rectus capitis posterior major m.*, rectus capitis posterior minor m.*, obliquus capitis superior m.*, obliquus capitis inferior m.*, digastric m.*, stylohyoid m.*, mylohyoid m.*, geniohyoid m.*, sternohyoid m.*, omohyoid m.*, sternothyroid m.*, thyrohyoid m.*
	Muscles of back	Trapezius m.*, latissimus dorsi m.*, rhomboid major m.*, rhomboid minor m.*, levator scapulae m.*, serratus posterior superior m.*, erector spinae m.*, iliocostalis m.*, iliocostalis lumborum m.*, longissimus m.*, longissimus cervicis m.*, longissimus capitis m.*, splenius capitis m.*, transversospinales m.*, semispinalis cervicis m.*, semispinalis capitis m.*
	Muscles of thorax	Pectoralis major m.*, pectoralis minor m.*, subclavius m.*, serratus anterior m.*, intercostal mm.*, diaphragm
	Muscles of abdomen	Rectus abdominis m.*, external oblique abdominal m.*, internal oblique abdominal m.*, transversus abdominis m.*, quadratus lumborum m.*, levator ani m., coccygeus m.*
	Muscles of upper limb	Deltoid m.*, supraspinatus m.*, infraspinatus m.*, teres minor m.*, teres major m.*, subscapularis m.*, biceps brachii m.*, coracobrachialis m.*, brachialis m.*, triceps brachii m.*, anconeus m.*, pronator teres m.*, flexor carpi radialis m.*, palmaris longus m.*, flexor carpi ulnaris m.*, flexor digitorum superficialis m.*, flexor digitorum profundus m.*, flexor pollicis longus m.*, pronator quadratus m.*, brachioradialis m.*, extensor carpi radialis longus m.*, extensor carpi radialis brevis m.*, extensor digitorum m.*, extensor digiti minimi m.*, extensor carpi ulnaris m.*, supinator m.*, abductor pollicis longus m.*, extensor pollicis brevis m.*, extensor pollicis longus m.*, extensor indicis m.*, palmaris brevis m.*, abductor pollicis brevis m.*, flexor pollicis brevis m.*, opponens pollicis m.*, adductor pollicis m.*, abductor digiti minimi m.*, flexor digiti minimi brevis m.*, opponens digiti minimi m.*, lumbrical mm.*, dorsal interossei mm.*, palmar interossei mm.*
	Muscles of lower limb	Iliopsoas m.*, iliacus m.*, psoas major m.*, gluteus maximus m.*, gluteus medius m., gluteus minimus m., tensor fasciae latae m.*, piriformis m.*, obturator internus m.*, superior gemellus m., inferior gemellus m., quadratus femoris m.*, sartorius m.*, rectus femoris m.*, vastus lateralis m.*, vastus intermedius m.*, vastus medialis m.*, articularis genus m.*, pectineus m.*, adductor longus m.*, adductor brevis m.*, adductor magnus m.*, gracilis m.*, obturator externus m.*, biceps femoris m.*, semitendinosus m.*, semimembranosus m.*, anterior tibialis m.*, extensor digitorum longus m., extensor hallucis longus m.*, fibularis longus m.*, fibularis brevis m.*, gastrocnemius m.*, soleus m.*, plantaris m.*, popliteus m.*, posterior tibialis m.*, flexor digitorum longus m.*, flexor hallucis longus m., extensor digitorum brevis m.*, abductor hallucis m.*, flexor hallucis brevis m.*, adductor hallucis m. oblique head*, adductor hallucis m. transverse head*, abductor digiti minimi m.*, flexor digiti minimi brevis m.*, flexor digitorum brevis m.*, quadratus plantae m.*, plantar interossei m.*

Table 1 continued

System	Classification	Structure
Alimentary (75)	Salivary glands	Parotid gland*, sublingual gland*, submandibular gland*
	Teeth[a]	Medial maxillary incisor tooth*, lateral maxillary incisor tooth*, maxillary canine tooth*, first maxillary premolar tooth*, second maxillary premolar tooth*, first maxillary molar tooth*, second maxillary molar tooth*, medial mandibular incisor tooth*, lateral mandibular incisor tooth*, mandibular canine tooth*, first mandibular premolar tooth*, second mandibular premolar tooth*, first mandibular molar tooth*, second mandibular molar tooth*
	Tongue	Tongue, genioglossus m.*, hyoglossus m.*, styloglossus m.*, palatoglossus m.*
	Fauces	Soft palate, tensor veli palatini m., levator veli palatini m.
	Pharynx	Pharynx, constrictor mm., stylopharyngeus m.*
	Esophagus, Stomach[b]	Esophagus (mural), esophagus (luminal), stomach (mural), stomach (luminal)
	Small intestine (mural)[b]	Duodenum, jejunum and ileum
	Large intestine (mural)[b]	Cecum, appendix, ascending colon, transverse colon, descending colon, sigmoid colon, rectum, anal canal, external anal sphincter m.
	Liver[c]	Liver, common hepatic duct (luminal), right hepatic duct (luminal), left hepatic duct (luminal)
	Gallbladder (luminal)[c]	Gallbladder, cystic duct, common bile duct, hepatopancreatic ampulla
	Pancreas[c]	Pancreas, pancreatic duct (luminal)
Respiratory (43)	Nose (luminal)[d]	Nasal cavity, maxillary sinus*, sphenoidal sinus*, frontal sinus, ethmoidal cells
	Larynx[d]	Larynx, Cricothyroid m.*, Posterior crico-arytenoid m.*, Lateral crico-arytenoid m.*
	Trachea (luminal)[d]	Trachea
	Bronchi (luminal)[d]	Right main bronchus, right superior lobar bronchus, right apical segmental bronchus, right posterior segmental bronchus, right anterior segmental bronchus, right middle lobar bronchus, right lateral segmental bronchus, right medial segmental bronchus, right inferior lobar bronchus, right superior segmental bronchus, right medial basal segmental bronchus, right anterior basal segmental bronchus, right lateral basal segmental bronchus, right posterior basal segmental bronchus, left main bronchus, left superior lobar bronchus, left apicoposterior segmental bronchus, left anterior segmental bronchus, left superior lingular segmental bronchus, left inferior lingular segmental bronchus, left inferior lobar bronchus, left superior segmental bronchus, left medial basal segmental bronchus, left anterior basal segmental bronchus, left lateral basal segmental bronchus, left posterior basal segmental bronchus
	Lungs[e]	Lung*
Urinary (10)	Kidneys	Kidney*
	Ureters (mural)[f]	Ureter*
	Urinary bladder[f]	Urinary bladder (mural), urinary bladder (luminal)
	Urethra	Preprostatic part of urethra, prostatic urethra, intermediate part of urethra, spongy urethra
Genital (20)	Male internal genitalia[f]	Testis*, epididymis (mural)*, ductus deferens (mural)*, seminal vesicle (mural)*, ejaculatory duct (mural), prostate
	Male external genitalia	Corpora cavernosa penis*, corpus spongiosum penis, superficial transverse perineal m.*, ischiocavernosus m.*, bulbospongiosus m., deep transverse perineal m., external urethral sphincter m.
Endocrine (3)	Endocrine glands	Adenohypophysis, neurohypophysis, thyroid gland

Table 1 continued

System	Classification	Structure
Cardiovascular (luminal)[g] (138)	Heart	Heart (mural), pericardial cavity, right ventricle, right atrium, tricuspid valve, pulmonary valve, left ventricle, left atrium, mitral valve, aortic valve
	Pulmonary trunk[h]	Pulmonary trunk, pulmonary a.*
	Ascending aorta	Ascending aorta, right coronary a., sinu-atrial nodal branch, posterior interventricular branch, atrioventricular nodal branch, left coronary a., anterior interventricular branch, circumflex branch, left marginal a.
	Arch of aorta	Arch of aorta, brachiocephalic trunk, common carotid a.*, external carotid a.*, internal carotid a.*, subclavian a.*, vertebral a.*, basilar a., axillary a.*, brachial a.*, deep brachial a.*, radial a.*, ulnar a.
	Descending aorta	Descending aorta, celiac trunk, left gastric a., common hepatic a., gastroduodenal a., proper hepatic a., cystic a., splenic a., superior mesenteric a., inferior mesenteric a., common iliac a.*, internal iliac a.*, lliolumbar a., obturator a.*, superior gluteal a.*, inferior gluteal a.*, inferior vesical a.*, internal pudendal a.*, external iliac a.*, inferior epigastric a., femoral a.*, deep femoral a.*, popliteal a.*, anterior tibial a.*, posterior tibial a.*
	Coronary sinus	Coronary sinus, great cardiac v., middle cardiac v., small cardiac v.
	Pulmonary veins[h]	Superior pulmonary v.*, inferior pulmonary v.*
	Superior vena cava	Superior vena cava, brachiocephalic v.*, internal jugular v.*, transverse sinus*, confluence of sinuses, occipital sinus, sigmoid sinus*, superior sagittal sinus, inferior sagittal sinus, straight sinus, subclavian v.*, axillary v.*, brachial v.*, basilic v.*, cephalic v.*, azygos v., hemi-azygos v., accessory hemi-azygos v.
	Inferior vena cava	Inferior vena cava, right hepatic v., intermediate hepatic v., left hepatic v., renal v.*, common iliac v., internal iliac v.*, external iliac v.*, great saphenous v.*, small saphenous v.*, femoral v.*, popliteal v.*, superior mesenteric v., splenic v., inferior mesenteric v.
Lymphoid (1)	Lymphoid organs[i]	Spleen
Nervous (95)	Spinal cord	Spinal cord
	Brain	Brainstem, cerebellum, thalamus, frontal lobe*, parietal lobe*, occipital lobe*, temporal lobe*, fornix, lateral ventricle*, amygdaloid nucleus*, caudate nucleus*, putamen*, globus pallidus*, claustrum*
	Cranial nerves	Optic n.*
	Spinal nerves[j]	Brachial plexus*, median n.*, ulnar n.*, radial n.*, anterior root of first lumbar n.*, anterior ramus of first lumbar n.*, anterior root of second lumbar n.*, posterior root of second lumbar n.*, anterior ramus of second lumbar n.*, anterior root of third lumbar n., posterior root of third lumbar n., anterior ramus of third lumbar n., anterior root of fourth lumbar n.*, posterior root of fourth lumbar n.*, anterior ramus of fourth lumbar n.*, anterior root of fifth lumbar n., posterior root of fifth lumbar n.*, anterior ramus of fifth lumbar n.*, anterior root of first sacral n.*, posterior root of first sacral n.*, anterior ramus of first sacral n.*, anterior root of second sacral n.*, posterior root of second sacral n.*, anterior ramus of second sacral n.*, anterior root of third sacral n.*, posterior root of third sacral n.*, anterior ramus of third sacral n.*, superior gluteal n.*, inferior gluteal n.*, obturator n.*, femoral n.*, sciatic n.*, tibial n.*, common fibular n.*, superficial fibular n.*, deep fibular n.*
Sensory (22)	Eyes	Eyeball*, superior rectus m.*, inferior rectus m.*, medial rectus m.*, lateral rectus m.*, superior oblique m.*, inferior oblique m.*, levator palpebrae superioris m.*
	Ears	External acoustic meatus*, tympanic cavity*, auditory tube*

Table 1 continued

System	Classification	Structure
Integumentary (1)	Skin	Skin

System (Number of structures)

m. muscle, *mm.* muscles, *a.* artery, *v.* vein, *n.* nerve

* Bilateral structures

[a] The cadaver doesn't comprise the third maxillary and mandibular molar teeth in both sides

[b] In the digestive tract, esophagus and stomach are outlined along both mural, luminal contours: the rest parts are outlined along only mural contours

[c] Bile and pancreatic ducts are outlined along their luminal contours

[d] Respiratory tract is outlined along its luminal contour

[e] Both lungs have pneumonia caused by leukemia; normal lung parenchyma is compressed by pneumonia

[f] Urogenital tract is outlined along its mural contour; exception is the urinary bladder, whose mural and luminal contours are outlined

[g] All heart chambers and blood vessels are outlined along their luminal contours

[h] Pulmonary vessels are outlined from heart to both lung hila

[i] Spleen is large due to leukemia

[j] Roots of lumbar and sacral nerves are outlined from the first lumbar vertebra level to the intervertebral foramina or anterior sacral foramina. Anterior rami of lumbar and sacral nerves are outlined excluding posterior rami

Filling outlines with colors

Black-filled images do not show their neighboring structures. To allow for individual identification of such structures, the black color must be changed to different colors; images of different structures can then be combined. On Photoshop, the black-filled images were transformed into outlined images. Outlines of black-filled images were made automatically using the 'magic wand' tool (Fig. 4b).

On Photoshop, the outlined images were transformed into color-filled images. After changing the 2-bit color to 16-bit color, the outlines were filled in with colors using the 'fill' command (Fig. 4c). The outline of the skin was not filled in, only colored. RGB triplets for individual structures had already been determined (Table 2). At this time, the 'anti-aliased' option had to be turned off in order to prevent unintentional creation of intermediate colors. The background color of color-filled images was then changed transparently by deleting the background color.

On Photoshop, the color-filled images of all structures, at the same level, were combined using the 'load files into stack' command. This was possible because the backgrounds of color-filled images were kept transparent, not white (Fig. 4d). At this time, large structures might hide small internal structures, such as the heart hiding the right ventricle. To avoid this situation, some layers, including the structures' color-filled outlines, were rearranged. The combined color-filled images were saved as TIFF files without layers. Consequently, 1,702 color-filled images of 937 structures were prepared (Fig. 1b).

Sectioned images and color-filled images were stacked in order to generate coronal and sagittal planes on composed software (Fig. 5).

Volume reconstruction

A volume model for each structure was constructed using sectioned and black-filled images (Fig. 6a), as follows: on Photoshop, the black-filled images (TIFF files) of a structure were automatically converted back into outlined images (PSD files). Then, with the outlined images, the structure's surroundings were erased in the sectioned images (Fig. 6b). In 3D-DOCTOR (version 4; Able Software, Corp., Lexington, MA, USA), the sectioned images were stacked and reconstructed using the 'direct volume rendering' command in order to build a volume 3D model (Fig. 6c) [7, 16].

Surface reconstruction

The black-filled images of a structure were stacked sequentially using 3D-DOCTOR. Using the 'simple surface' command, the black-filled outlines were expanded to the next ones in order to build combined volume models, defined as volume reconstruction; simultaneously, from this expansion, a surface 3D model was extracted (surface reconstruction). The surface model, consisting of stacked outlines and polygons between outlines, was saved in the drawing exchange format (DXF). To smooth the surfaces, stacked outlines were deleted using the 'smooth' command

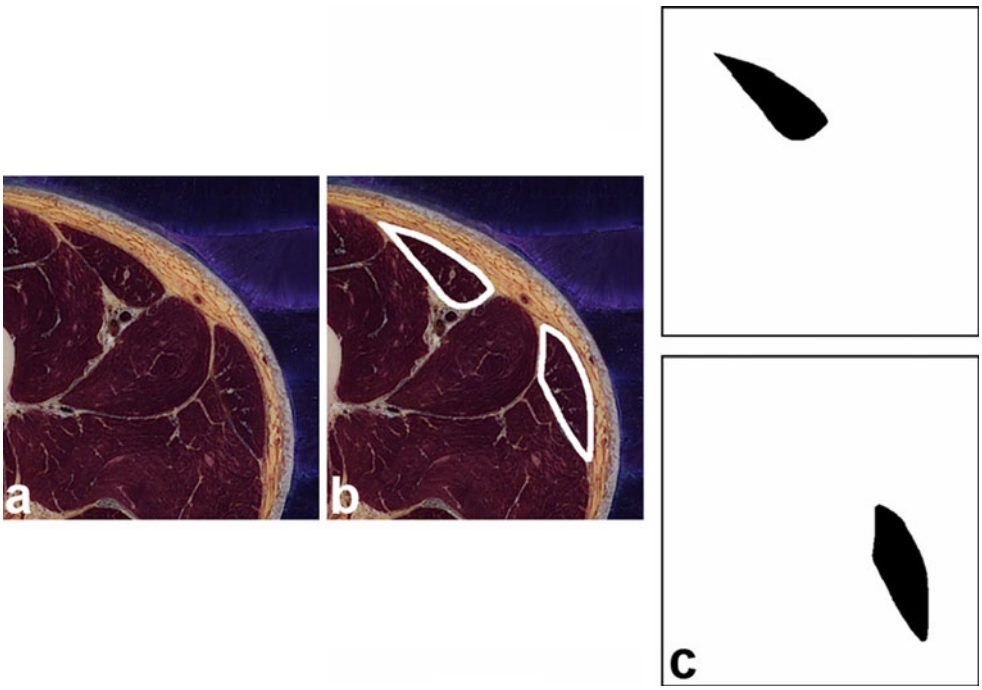

Fig. 2 **a** Sectioned image, **b** outlined image of the sartorius and gracilis muscles, and **c** *black-filled* images of the muscles

Table 2 Information on outlined structures

Structure	Side	Top image	Bottom image	RGB triplet		
Cranium without mandible		0035	1010	222	204	227
Mandible		0735	1250	92	92	79
…		…	…	…	…	…
First rib	Right	1435	1810	186	158	102
First rib	Left	1430	1795	224	214	181
…		…	…	…	…	…
Skin		0000	8505	153	51	51

of Maya (version 7.0; Autodesk, Inc., San Rafael, CA, USA), and the number of polygons was appropriately reduced using the 'reduce' command of Maya. The elaborated surface model was saved as a Maya binary (MB) file [8, 16].

In the new MB file, the surface model of each structure was placed in its own layer to produce assembled surface models, which allowed for selective display of surface models of structures (Fig. 7) [15].

Results

In the present study, outlining was verified using different approaches. The black-filled images of each structure were displayed sequentially in order to look for extraordinarily large or small outlines among the series. Outlines that were absent or those overlapped with adjacent outlines at one level were easily found, as they interrupted the automatic conversion of black-filled images into combined color-filled images (Fig. 4). Almost incorrect outlines in coronal and sagittal color-filled images could not be overlooked (Fig. 5b, d). Even after reconstruction, we were verifying

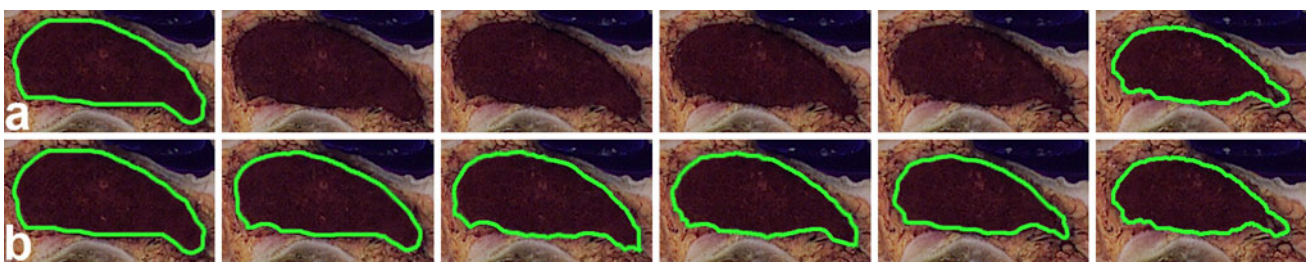

Fig. 3 **a** Sectioned images at 0.2 mm intervals, the first and last of which are already outlined along the spleen and **b** the middle four outlines are created by interpolation

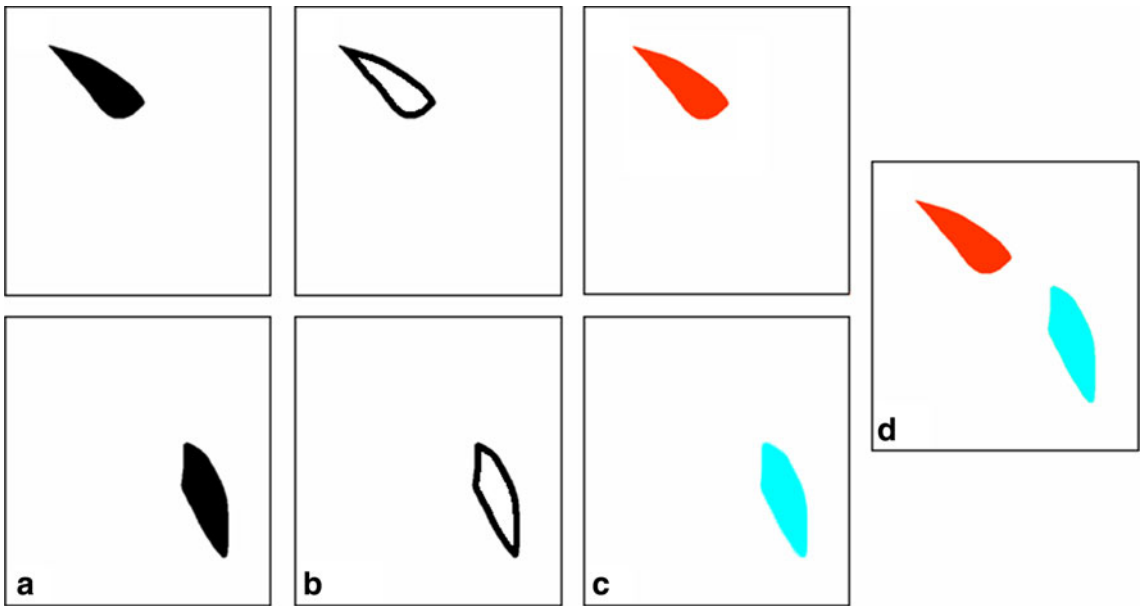

Fig. 4 **a** *Black-filled* images, **b** outlined images, **c** *color-filled* images, and **d** *combined color-filled* image of the sartorius and gracilis muscles

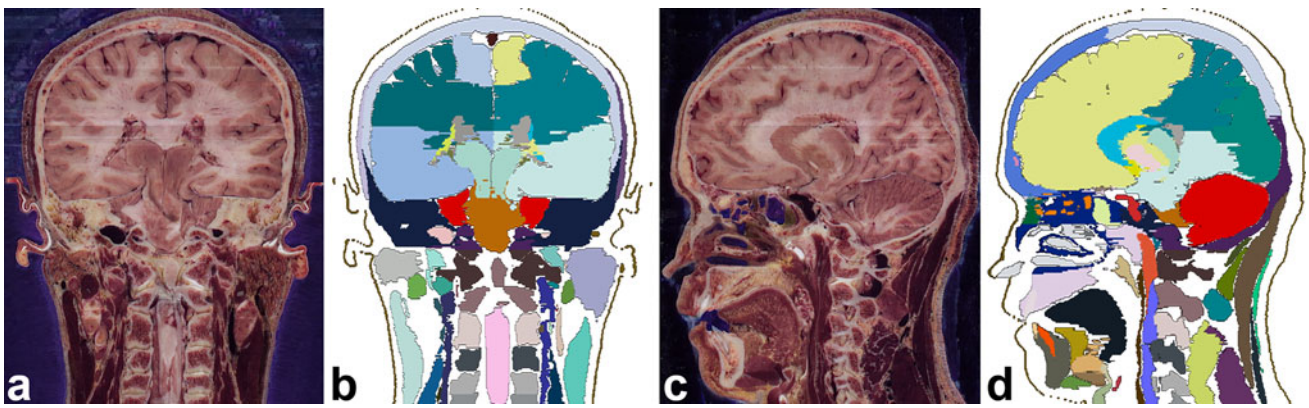

Fig. 5 **a** Coronal sectioned image, **b** *coronal color-filled* image, **c** sagittal sectioned images, and **d** *sagittal color-filled* images of head structures

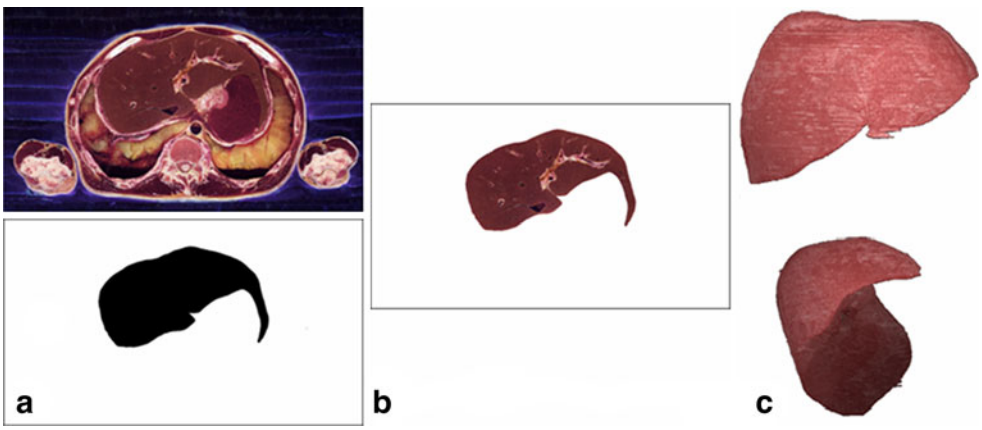

Fig. 6 **a** Sectioned image and *black-filled* image of the liver, **b** sectioned image with surrounding tissues erased, and **c** a volume model of the liver

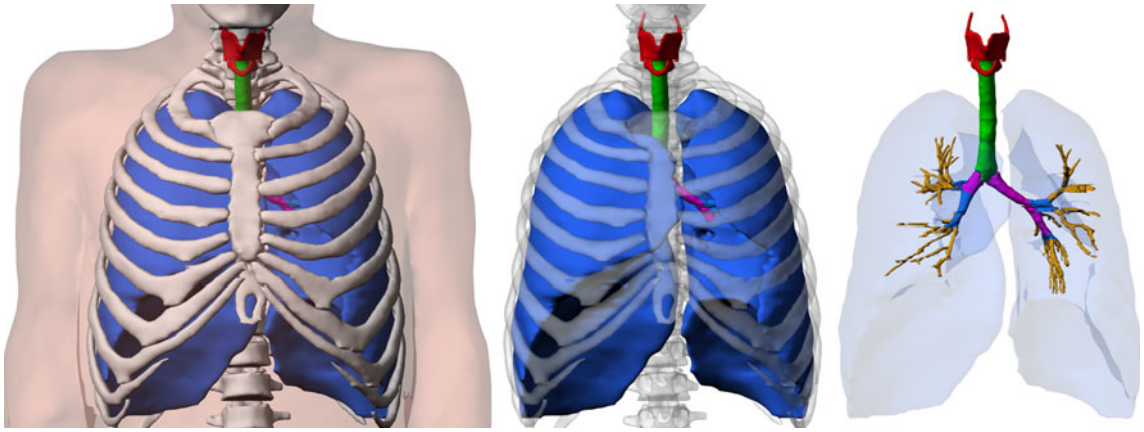

Fig. 7 Surface models of the respiratory organs and neighboring structures, displayed differently

incorrect outlines remained. Neighboring volume and surface models were selected for display and were rotated for investigation of inappropriate stereoscopic shape of the structures, caused by incorrect outlining (Figs. 6c, 7) [11]. Volume models of bones were compared with those reconstructed from CT images of the same cadaver for identification of mistaken outlining of bones; this method was useful because bones are outlined automatically in CT images. In cases where incorrect outlining was detected, the outlined images were revised as far as we could confirm the accuracy.

The main outcome of this research was the construction of novel black-filled images. Users who were informed by the list (Table 1) could easily find the appropriate folders where the required black-filled images had been placed. In particular, medical doctors familiar with standard anatomy terms could easily select folders, set up on the basis of Terminologia Anatomica [3].

The 'Skin' folder contained 1,702 black-filled images (TIFF files), whereas the other folders contained fewer images (Table 2). In total, 937 folders included 81,459 black-filled images. File sizes of one black-filled image and of the 81,459 images were 3 MB and 268 GB, respectively. After compression into the Roshal archive format, the file sizes were 6 KB and 587 MB, respectively. Sectioned images corresponding to the black-filled images were the ones requested by users. File sizes of one sectioned image and of the 1,702 images were 18 MB and 29 GB, respectively. Sectioned images with true color were minimally compressed.

Color-filled images, derived from the black-filled images, were useful. They could be used for identification of structures in the corresponding sectioned images (Fig. 1). After programming, the names of the outlined structures could be displayed using the structure's RGB triplet (Table 2) [14].

Black-filled images with sectioned images could be used to build 3D volume models (Fig. 6). The top and bottom information on the black-filled images could be helpful to investigators in design of a volume model of a structure (Table 2). Volume models could be arbitrarily sectioned to display sectional planes in anatomical colors [13].

Black-filled images, excluding sectioned images, could be used in generation of surface 3D models, and the surface models could be selected for display (Fig. 7), rotated, and modified in real time, thanks to the small file sizes, which are essential for interactive medical simulations [16].

Discussion

The Visible Korean data have been distributed as an educational tool for use by medical students and as interactive clinical simulation systems for use by medical doctors. Initially, only sectioned images from the Visible Korean were presented in the expectation that users would outline structures in the sectioned images for their own specific purposes. However, users wanted to be supplied with the outlined images. In order to reduce repetitive and tedious work, we decided to offer not only sectioned images but also corresponding outlined images. To satisfy various investigators with different objectives, we outlined a large number of body structures (Table 1).

Outlining of the sectioned images cannot be done automatically. In the medical imaging field, a variety of algorithms for automation of outlining have been developed [2, 4–6]. However, the algorithms usually fit clinical images, such as CT and MR images, not sectioned images with 24-bit color and high resolution. And, some open source algorithms (e.g., ITK, insight segmentation and registration tool kit) are not readily available for this project without programming. Another reason that automatic

outlining is not practical is the detail of the structures involved. For example, neighboring muscles cannot be separated graphically in sectioned images; therefore, their borders have to be drawn interactively by experts in human anatomy. Thus, inevitably, outlining is a time-consuming task. For a complete cadaver, MR and CT images were scanned over a period of a few hours, and the serial sectioning took 3 months [13]. However, outlining of 937 structures in 1,702 sectioned images required 8 years (Table 1).

Structures in sectioned images can be outlined efficiently using commercial photo-editing software, which frees investigators from programming [7, 12]. These software packages have many functions, which can semi-automate outlining when optimally used. Example is image filtering on Photoshop and interpolation with Combustion (Fig. 3). These software packages are continuously upgraded and are equipped with additional functions. For example, the new tool 'quick selection' on the recent version of Photoshop (CS3) can be employed for efficient outlining. This technique can be reproduced by other investigators for creation of their own outlined images. In addition, popular software, such as the 3D-DOCTOR and Maya, can be used for volume and surface reconstruction independent of computer programmers [7, 8, 16]. Instead, we expect that programmers will use the Visible Korean data for development of educational programs as the end products.

After outlining, a significant issue was the file format to use for distribution. In a previous report, PSD files were preferred for distribution because, using 'actions' and 'batch' in Photoshop, all outlined images could be simultaneously transformed into black-filled images or color-filled images of the selected structures (Figs. 2, 4). In a previous report, all PSD files included only 13 layers of 13 outlined structures [12]; however, in this report, each file had 937 layers. Users who want only skin outlines should select skin layers among the 937 layers in the PSD files. By contrast, TIFF files of black-filled images of skin, already arranged in the 'Skin' folder, can be selectively obtained, and conveniently utilized. In addition, due to many layers, one PSD file is very large (86 MB), and a layer in the PSD file requires a larger file size (95 KB) than a compressed TIFF file (6 KB) in only 2-bit color. Therefore, TIFF or a similar file format is appropriate for off-line or even on-line distribution [15].

From the TIFF files of the black-filled images, PSD files of outlined images can be automatically produced; therefore, there is no difference in availability between TIFF files and PSD files. For example, with PSD files, interpolation, filling of outlines, and erasing tissue outside a structure can be done for acquisition of interpolated images (Fig. 3b), color-filled images (Fig. 4d), and volume model (Fig. 6c), respectively.

Even though more than 900 structures have been outlined, much remains to be done. Users can now outline additional structures as needed. Although the outlines were drawn by medical experts, and incorrect outlines were revised after verification, some errors are inevitable. Users should amend the errors after considering the original sectioned images. In addition, as users share the added and amended outlines, the Visible Korean data will be progressively upgraded. We hope that this continuous improvement will establish a virtual image library of the Visible Korean.

In order to enhance the values of the outlined images, they need to be accompanied by appropriate sectioned images and 3D models. In addition, corresponding MR and CT images of the same cadaver can be used for production of useful software [13]. For example, surface models can be superimposed on sectioned, color-filled, or CT images to aid in stereoscopic comprehension of the structures.

Our policy on distribution of contents has been welcomed by investigators. A variety of educational tools, including virtual dissection, virtual endoscopy, and virtual lumbar puncture have been developed using Visible Korean data [14–16, 22]. In addition, volume 3D models based on the Visible Korean have been used for virtual exposure to radiation for calculation of the dosimetry of vital and radiosensitive organs [9].

This research used sectioned images of a male cadaver. In 2010, we prepared images of a complete female cadaver. The intention will be to obtain outlines of female cadavers, no matter how many years the job takes. Data sets from both sexes will hopefully contribute to the medical imaging field in many different ways.

Acknowledgments This research was supported by Basic Science Research Program through the National Research Foundation of Korea (NRF) funded by the Ministry of Education, Science and Technology (Grant number 2010-0009950).

References

1. Ackerman MJ (1998) The Visible Human Project. Proc IEEE 86:504–511
2. Chen Y, Zhang J, Heng PA, Xia D (2008) Chinese Visible Human brain image segmentation. In: Proceedings of the 2008 Congress on Image and Signal Processing, pp 639–643
3. FCAT (Federative Committee on Anatomical Terminology) (1998) Terminologia Anatomica: International Anatomical Terminology. Thieme, Stuttgart, New York
4. Flores JM, Schmitt F (2005) Segmentation, reconstruction and visualization of the pulmonary artery and the pulmonary vein from anatomical images of the Visible Human Project. In: Proceedings of the Sixth Mexican International Conference on Computer Science, pp 136–144
5. Ghosh P, Mitchell M (2006) Segmentation of medical images using a genetic algorithm. In: Proceedings of the 8th Annual Conference on Genetic and Evolutionary Computation Table of Contents, pp 1171–1178

6. Grau V, Mewes AUJ, Alcañiz M et al (2004) Improved watershed transform for medical image segmentation using prior information. IEEE Trans Med Imaging 23:447–458
7. Huang YX, Jin LZ, Lowe JA et al (2010) Three-dimensional reconstruction of the superior mediastinum from Chinese Visible Human female. Surg Radiol Anat 32:693–698
8. Jang HG, Chung MS, Shin DS et al (2011) Segmentation and surface reconstruction of the detailed ear structures, identified in sectioned images. Anat Rec 294:559–564
9. Kim CH, Jeong JH, Bolch WE et al (2011) A polygon-surface reference Korean male phantom (PSRK-Man) and its direct implementation in Geant4 Monte Carlo simulation. Phys Med Biol 56:3137–3167
10. Lou L, Liu SW, Zhao ZM et al (2009) Segmentation and reconstruction of hepatic veins and intrahepatic portal vein based on the coronal sectional anatomic dataset. Surg Radiol Anat 31:763–768
11. Park JS, Chung MS, Chi JG et al (2010) Segmentation of cerebral gyri in the sectioned images by referring to volume model. J Korean Med Sci 25:1710–1715
12. Park JS, Chung MS, Hwang SB et al (2005) Technical report on semiautomatic segmentation by using the Adobe Photoshop. J Digit Imaging 18:333–343
13. Park JS, Chung MS, Hwang SB et al (2005) Visible Korean Human: improved serially sectioned images of the entire body. IEEE Trans Med Imaging 24:352–360
14. Park JS, Jung YW, Lee JW et al (2008) Generating useful images for medical applications from the Visible Korean Human. Comput Methods Programs Biomed 92:257–266
15. Shin DS, Chung MS, Park JS et al (2010) Three-dimensional surface models of detailed lumbosacral structures reconstructed from the Visible Korean. Ann Anat 193:64–70
16. Shin DS, Park JS, Lee SB et al (2009) Surface model of the gastrointestinal tract constructed from the Visible Korean. Clin Anat 22:601–609
17. Spitzer VM, Ackerman MJ, Scherzinger AL (2006) Virtual anatomy: an anatomist's playground. Clin Anat 19:192–203
18. Spitzer VM, Ackerman MJ, Scherzinger AL et al (1996) The Visible Human male: a technical report. J Am Med Inform Assoc 3:118–130
19. Sun B, Tang YC, Fan LZ et al (2008) The pineal region: thin sectional anatomy with MR correlation in the coronal plane. Surg Radiol Anat 30:575–582
20. Tang L, Chung MS, Liu Q et al (2010) Advanced features of whole body sectioned images: Virtual Chinese Human. Clin Anat 23:523–529
21. Tang YC, Zhao ZM, Lin XT et al (2009) The thin sectional anatomy of the sellar region with MRI correlation. Surg Radiol Anat 32:573–580
22. Uhl JF, Park JS, Chung MS et al (2006) Three-dimensional reconstruction of urogenital tract from Visible Korean Human. Anat Rec A Discov Mol Cell Evol Biol 288:893–899
23. Wu Y, Zhang SX, Na Luo et al (2010) Creation of the digital three-dimensional model of the prostate and its adjacent structures based on Chinese Visible Human. Surg Radiol Anat 32:629–635
24. Yuan Y, Qi L, Luo S (2008) The reconstruction and application of Virtual Chinese Human female. Comput Methods Programs Biomed 92:249–256
25. Zhang SX, Heng PA, Liu ZJ (2006) Chinese Visible Human Project. Clin Anat 19:204–215
26. Zhen JP, Liu C, Wang SY et al (2007) The thin sectional anatomy of the temporal bone correlated with multislice spiral CT. Surg Radiol Anat 29:409–418